

# Synthesis and Characterization of Ni-Zn-Fe Alloy as an Electrocatalyst for Alkaline Water Electrolysis

Rugi Vicente Del Castillo Rubi<sup>1,\*</sup>, Marie Angelynne Fabro<sup>2</sup>, Milton Bianda Dela Rosa Jr.<sup>1</sup>, Maria Angelica Abello Diongson<sup>1</sup>, Gee Hyun Lee<sup>1</sup>, Angelica Ramos Mondala<sup>1</sup>, Kathleen May Rubio Piamonte<sup>1</sup>, and Nur Laila Hamidah<sup>3</sup>

<sup>1</sup>Department of Chemical Engineering, College of Engineering, Adamson University, 900 San Marcelino, Ermita, Manila 1000, Philippines

<sup>2</sup>Material Science Engineering Department, College of Engineering, University of the Philippines, Roxas Ave, Diliman, Quezon City, Metro Manila, 1101, Philippines

<sup>3</sup>Department of Engineering Physics, Institut Teknologi Sepuluh Nopember, Jl. Arif Rahman Hakim, Keputih, Sukolilo, Surabaya, East Java, 60111, Indonesia

**Abstract.** Binary alloy of metals is an effective catalyst for hydrogen evolution using water electrolysis. The development of non-noble and low-cost material is very promising used as catalysis. Here, this work focuses on the electrodeposition of Ni-Fe-Zn as electrocatalyst for alkaline water electrolysis. Ni-Zn-Fe was deposited using co-deposition method at various potentials and plating times. The produced electrocatalyst was characterized using X-ray diffraction spectroscopy, and scanning electron microscope. Cyclic voltammetry (CV) was used to characterize the electrochemical behaviour of the alloy in 1.0 M KOH. The metaphase of Ni-Zn-Fe alloys showed in XRD spectra which present the electrodeposits of metal alloys. The SEM spectra captured the agglomerates particle with rougher morphology and larger surface area which highly desirable for solid catalysts. Electrodeposition of the alloy showed that for every increase in voltage corresponds to an increase of 0.12 607 on the mass deposit. CV scan showed the hydrogen oxidation process. The forward and backward passes follow the same trace which indicates that no other reaction is taking place during the first CV scan. These results indicate the excellent catalytic activity of Ni-Zn-Fe electrocatalyst for bright prospect of hydrogen production by alkaline water electrolysis.

**Keywords:** Cyclic voltammetry, electrodeposition, hydrogen generation, ternary alloy

## 1 Introduction

Hydrogen energy has fascinating potential for various industrial applications. Hydrogen is seen by many as an energy carrier, similar to electricity, which can be produced in one place and consumed somewhere else [1]. However, hydrogen does not exist in nature as a gas, and the production of hydrogen is primarily manufactured by steam reforming of natural gas which emitted a carbon footprint [2]. The hydrogen generation from water electrolysis is a promising alternative to the carbon-emitting natural gas-based energy plant [3, 4]. The development of non-noble and low-cost material hydrogen production via alkaline water electrolysis is significantly required but remains a challenge. The most common electrocatalysis used for hydrogen evolution reaction (HER) is Pt-group metals

\* Corresponding author: [rugi.vicente.rubi@adamson.edu.ph](mailto:rugi.vicente.rubi@adamson.edu.ph)

due to its high activity by its close-to-thermoneutral hydrogen binding energy [5,6]. However, they required a high cost for massive production [7]. The operation in alkaline solution opens the potential of the usage of non-noble metal electrocatalyst leading to the economic hydrogen production. Therefore, the utilization of the candidate's non-precious metal catalysis with similar strength and activity gained much interest.

Nickel and its alloys are known to show high catalytic activity for HER [8,9]. Furthermore, enhancing the active area of the electrocatalyst by alloying with elements through the synergistic effect leads to an increase the power efficiency [10]. Among other metals, Iron (Fe) has been used as alloy for nickel because of its high hydrogen adsorption characteristic. On other hand, Zinc (Zn) is a unique amphoteric element that is chemically active if it is alloyed with other material [10–12]. Hence, the electrodeposition of Ni-Fe-Zn as electrocatalyst for alkaline water electrolysis becomes the main focus of this study. Ni-Zn-Fe electrocatalyst was deposited using co-deposition method at various potentials and plating times. The phase and crystalline size of the Ni-Zn-Fe alloy coating were characterized by X-ray Diffraction (XRD) analysis. The surface morphology of the alloy electrocatalyst was studied using Scanning Electron Microscope (SEM). Finally, cyclic voltammetry was used to characterize the electrochemical behavior of the alloy in 1.0 M KOH.

## **2 Material and method**

### **2.1 Mild steel substrate polishing and electro cleaning**

Mild Steel substrates with dimensions 1 cm × 1 cm were polished to a smooth finish using emery paper. Copper wire was soldered at the back of each substrate and covered with chemical and heat-resistant epoxy to ensure that only 1 cm<sup>2</sup> of the substrate is exposed. Each substrate was then washed with acetone prior to electro cleaning. A degreasing bath is used during the electro cleaning process. Under room temperature condition, each mild steel was cathodically cleaned by passing 3V for 3 min using platinum foil as anode with total exposed area of 1 cm<sup>2</sup>. This step was important because it removed oxides, oil, and contaminants that could hinder good deposition of metal. Finally, substrates were thoroughly washed with distilled water and dried. The mass of each dried substrate was determined using analytical balance.

### **2.2 Ni-Zn-Fe electrodeposition**

The electrodeposition of Zn-Ni-Fe was done at a constant temperature of 32 °C and pH of 3.5. The pH was monitored and adjusted by using either dilute hydrochloric acid (HCl) or ammonium hydroxide (NH<sub>4</sub>OH) depending on the requirement. Mild steel substrate was on the cathode side and pure Zinc plate of same geometrical area was on anode; maintaining a separation of 3 cm which is essential to minimize the voltage drop in the set-up. Stirring rate of 300 rpm (1 rpm = 1/60 Hz) was maintained to provide similar mass transfer. The potential was supplied by adjustable power source. The optimum voltage and optimum time of electrodeposition that gave good quality of deposit and electrocatalytic activity were determined by varying the voltage at 1.2 V to 2.2 V. Plated substrates were washed several times with distilled water to remove adhering solution, later dried, and then desiccated until further testing.

## 2.3 Ni-Zn-Fe coating and electrochemical characterization

X-Ray Diffraction (XRD) technique was used to determine the phase and crystalline size of the Ni-Zn-Fe alloy coating. The surface morphology of the best electrocatalyst for hydrogen evolution was analyzed by utilizing scanning Electron Microscope (SEM). All characterizations were carried out using three-electrode set-up. The platinum electrode of 1.0 cm<sup>2</sup> surface, electrodeposited Ni-Zn-Fe and Saturated Calomel Electrode (SCE) were utilized as counter, working and standard electrode respectively. Luggin's capillary with KCl Bridge was employed to eliminate the error due to IR drop. The distance between Ni-Zn-Fe and Platinum was maintained at approximately 1 cm. All electrochemical measurement was conducted at room temperature. Electrochemical measurements include Cyclic Voltammetry (CV) in the hydrogen evolution region (HER) was conducted in 1.0 M potassium hydroxide (KOH).

## 3 Results and discussion

### 3.1 Ni-Zn-Fe coatings crystallinity and morphological analysis

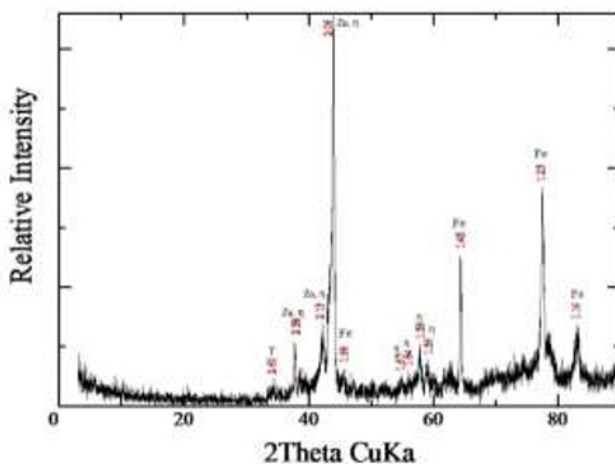


**Fig.1** XRD patterns of Ni-Zn-Fe coating on mild steel at 1.7 V and 15 min.

Figure 1 shows the XRD patterns of Ni-Zn-Fe coatings on the mild steel substrate. X-ray diffraction is a quantitative analysis based on diffractive intensities to determine the phase composition of the coatings [13]. Metastable phases are usually present to the electrodeposits; these are the phases that are either lacking or oversaturated of deposits compared to their corresponding parts in [14]. The electrodeposits of Ni-Zn-Fe alloys,  $\eta$  phase and  $\gamma$  phase are present. The  $\eta$  phase is the solid solution of Ni in Zn while  $\gamma$  phase is an intermetallic compound that has the formula of Ni<sub>5</sub>Zn<sub>21</sub> [15]. Based on Figure, the reflection of the pattern of Ni-Zn-Fe coatings belongs to the mild steel substrate, also of the major  $\eta$  phase and minor  $\gamma$  phase with crystal orientation.

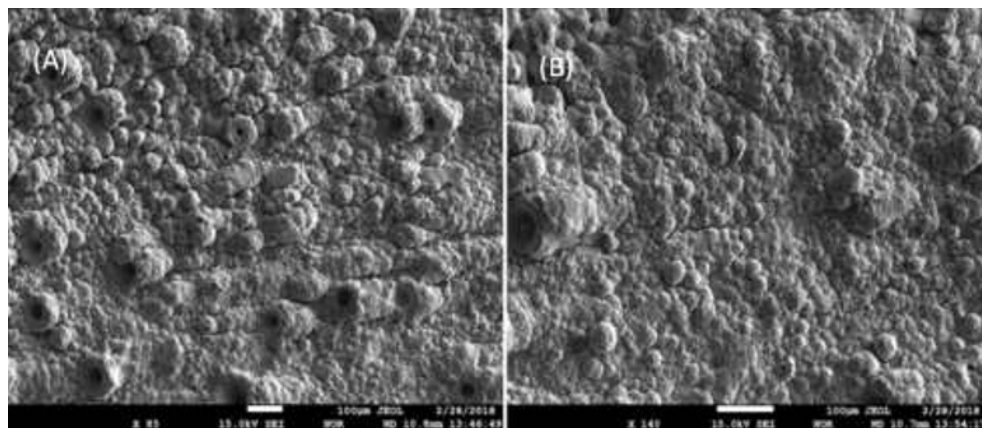


**Fig. 2** SEM image of Ni-Zn-Fe electrodeposited at 1.7 V and 15 min taken at A) 85x B) 140x.

The SEM image of the electrocatalyst is shown above. It can be seen the deposit consists of agglomerated particles. It contributes to a rougher morphology for this type of catalyst. Therefore, the real surface area is actually larger than the geometric surface area. It is highly desirable for solid catalysts because it offers larger area for surface reaction. Ternary alloys of iron and nickel exhibit unusual nucleation which results to highly coordinated adion that can initiate larger agglomerates that translates to a rougher structure.

### 3.2 The effect of voltage and plating time on mass deposited

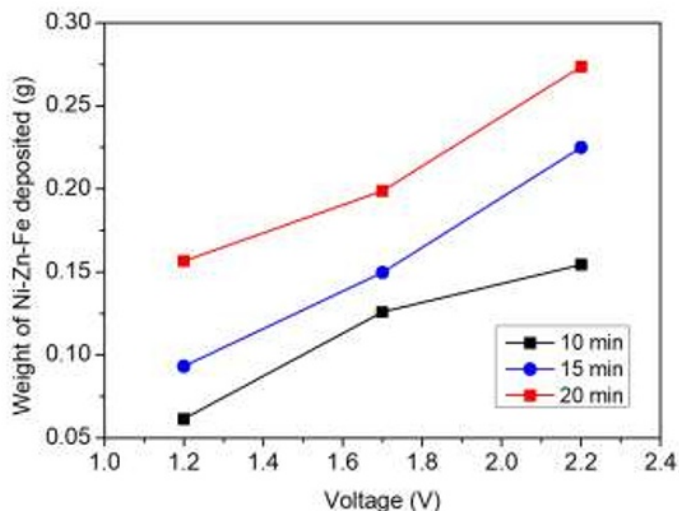


**Fig. 3** The effect of voltage on the amount of Ni-Zn-Fe deposits at a given time.

The determination of the effects of the deposition time and plating voltage on the amount of Ni-Zn-Fe deposit was analyzed through a full 32 factorial design experiment with three replications. To give a more accurate analysis, Ni-Zn- Fe plating bath was freshly prepared for every deposition. Figure 3 illustrates the effect of voltage on the amount of weight deposited on the mild steel substrate for the three trials. Based on the graph, at a given time, the weight of substance deposited for every substrate increases as the voltage used in electrodeposition increases. In accordance to Ohm's Law, voltage is directly proportional to the current flowing in the system. At constant resistance, an increase in voltage would give an increase in the flow of current. Furthermore, the electrodeposition on the substrate obeys Faraday's Law of electrolysis wherein mass deposited increases with increasing current. The current is proportional to the rate of plating. The higher current flowing in the system is the faster deposition. Hence, at constant time, higher amount is deposited at higher plating current.

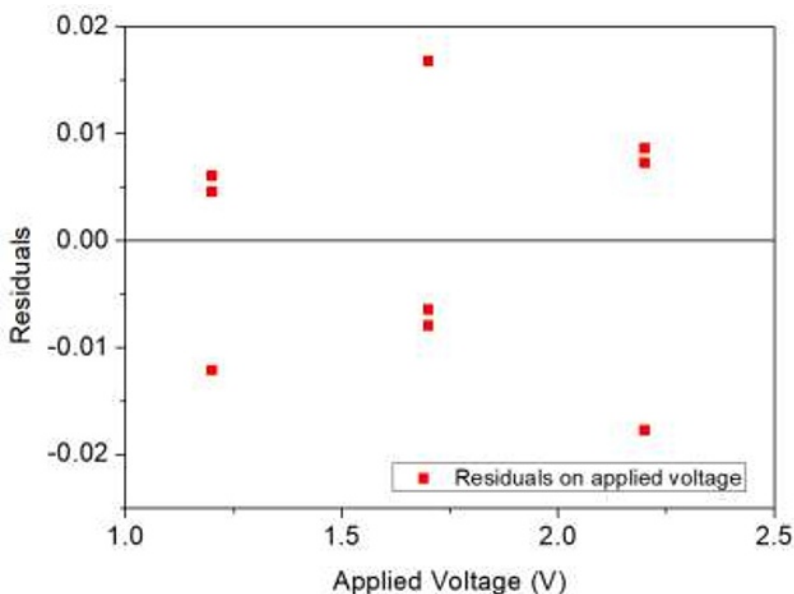


**Fig. 4** Residual plot of applied voltage.

The value for the  $R^2$  is at 0.96 377, indicating that the relationship of plating voltage on the weights deposited is 96.37 % well fitted on the line. 96.37 % of the variation in the amount of weight deposited is affected by the applied voltage. Moreover, the coefficients of voltage were 0.12 067. It suggests that an increase in the applied voltage will increase the amount of weight deposited by 0.12 067, on average. Hence, deposited weights on the substrate have direct proportionality in the plating voltage.

### 3.3 Cyclic voltammetry

Figure 5 shows the CV scan of Ni-Zn-Fe electrocatalyst deposited at 2.2 V and 20 min. Point 1 represents the oxygen adsorption step. The rapid rise of current to point 2 indicates the oxygen evolution at a potential of 1.02 V. A decreased in current was observed until point 3 which shows the oxygen reduction process. A scan to the negative potential until

point 4 reveals the hydrogen absorption step. Going to the more negative potential where there is a decrease in current shows that point 5 is the hydrogen evolution step at a potential at around -1.036 V. Point 6 illustrates the hydrogen oxidation process. The forward and backward passes follow the same trace which indicates that no other reaction is taking place during the first CV scan. It can be seen that similar onset potentials for hydrogen evolution were measured for the succeeding scans. The first three scans show same trace indicating that no other surface reactions occurring. However, it can be observed for the fourth and fifth scans exhibit hysteresis which shows that possible surface reactions are simultaneously occurring with gas evolution reaction. These results indicate the excellent catalytic activity of Ni-Zn-Fe electrocatalyst for the bright prospect of hydrogen production by alkaline water electrolysis.

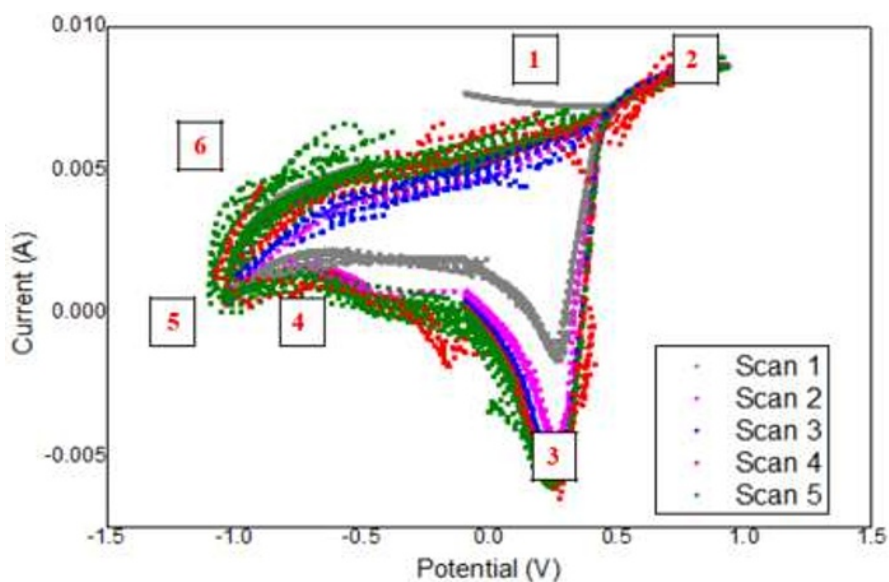


**Fig. 5** CV scan of catalyst CC (2.2V-20min) in 1.0 M KOH taken at  $25 \text{ mV s}^{-1}$ .

## 4 Conclusion

The synthesis of Ni-Zn-Fe electrocatalyst was done by electro-deposited using the co-deposition method at various potentials and plating times. The structural, morphological, and electrochemical characterization of Ni-Zn-Fe electrocatalyst was studied using, XRD, SEM, and cyclic voltammetry analysis. Results on the deposition process showed that voltage and plating time affected the mass of the metal deposit. Multiple linear regression revealed that every increase in the potential corresponds to an increase of 0.12 607 and on the mass deposit. XRD spectra confirm the metaphase of Ni-Zn-Fe electrodeposits of metal alloys. The SEM spectra show the agglomerates particle with rougher morphology which highly desirable for solid catalysts. Cyclic voltammetry was used to study the electrocatalytic activity of each metal catalyst. All of the catalysts showed no other surface reaction as confirmed by similar traces of the five CV scans. These results indicate the excellent catalytic activity of Ni-Zn-Fe electrocatalyst for the bright prospect of hydrogen production by alkaline water electrolysis.

The authors thank Engr. Maria Angelynn Fabro of the University of the Philippines-DMME for her knowledge and contribution to the research.

## References

1. K. Mazloomi, C. Gomes, *Renewable and Sustainable Energy Reviews*, **16**:3024–3033(2012).  
<https://www.sciencedirect.com/science/article/abs/pii/S1364032112001220>
2. V. Subramani, A. Basile, T.N. Veziroğlu, *Compendium of Hydrogen Energy*, Oxford: Woodhead Publishing (2015), p. 83–107.  
<https://www.elsevier.com/books/compendium-of-hydrogen-energy/subramani/978-1-78242-361-4>
3. D.V. Esposito, S.T. Hunt, Y.C. Kimmel, J.G. Chen, *J. Am. Chem. Soc.* **134**:3025–3033(2012). <https://pubs.acs.org/doi/abs/10.1021/ja208656v>
4. K. Rajeshwar, R. McConnell, S. Licht, *Solar hydrogen generation*, New York: Springer-Verlag (2008). <https://www.springer.com/gp/book/9780387728094>
5. P. Lindgren, G. Kastlunger, A. A. Peterson, *ArXiv Preprint ArXiv*, **1903.09903**: 1–20(2019). [shttps://arxiv.org/abs/1903.09903](https://arxiv.org/abs/1903.09903)
6. Z. Xing, Q. Liu, A. M. Asiri, X. Sun, *ACS Catal.* **5**,1:145–149(2015).  
<https://pubs.acs.org/doi/abs/10.1021/cs5014943>
7. Y. Nie, L. Li, and Z. Wei, *Chem. Soc. Rev.* **44**:2168–2201(2015).  
<https://doi.org/10.1039/C4CS00484A>
8. C. Lupi, A. Dell’Era, M. Pasquali, *International Journal of Hydrogen Energy*, **34**,5:2101–2106(2009).  
<https://www.sciencedirect.com/science/article/abs/pii/S0360319909000524>
9. G. Lu, P. Evans, G. Zangari, *Journal of the Electrochemical Society* **150**,5:A551(2003). <https://iopscience.iop.org/article/10.1149/1.1561629/>
10. J. Zhang, Y. Zhou, S. Zhang, S. Li, Q. Hu, L. Wang, L. Wang, F. Ma, *Scientific Reports* **8**:15071(2018). <https://www.nature.com/articles/s41598-018-33205-4>
11. M. Farsak, E. Telli, A.O. Yüce, G. Kardaş, *International Journal of Hydrogen Energy*, **42**:6455–6461(2017).  
<https://www.sciencedirect.com/science/article/abs/pii/S0360319916333675>
12. W. Badawy, H. Nady, G.A. El-Hafez, *Journal of Alloys and Compounds* **699**: 1146–1156(2017).  
<https://www.sciencedirect.com/science/article/abs/pii/S0925838816341421>
13. L. Zwell A. Danko, *Applied Spectroscopy Reviews* **9**:167–221(1975).  
<https://www.tandfonline.com/doi/abs/10.1080/05704927508081490>
14. A.C. Hegde, K. Venkatakrishna, N. Eliaz, *Surface and Coatings Technology* **205**:2031–2041(2010).  
<https://www.sciencedirect.com/science/article/abs/pii/S0257897210007516>
15. N. Eliaz, K. Venkatakrishna, A.C. Hegde, *Surface and Coatings Technology*, **205**:1969–1978(2010).  
<https://www.sciencedirect.com/science/article/abs/pii/S0257897210007267>